

Transmitters Location Optimization for Drug Delivery Systems

Keishla D. Ortiz-Lopez
Texas A&M University
College Station, TX, USA
keishla.ortiz4@tamu.edu

Mahima Agumbe Suresh
Texas A&M University
College Station, TX, USA
mahima.as@tamu.edu

Radu Stoleru
Texas A&M University
College Station, TX, USA
stoleru@cse.tamu.edu

ABSTRACT

Drug Delivery Systems (DDSs) are of vital importance to treat dangerous diseases, such as cancer. The goal of DDSs is to provide the required medication to the diseased area without affecting other healthy parts of the body. Most advanced DDSs use nanoparticles since they are able to cross biological barriers, but it has been shown that about 1% of injected nanoparticles are delivered to the diseased area. Molecular Communication (MC) paradigm is used to study DDSs, in particular to model the propagation of nanoparticles by advection and diffusion throughout the cardiovascular system in order to maximize the amount of nanoparticles reaching the diseased area. While existing work proposes different methods to tackle this problem, none of them aim to identify the optimal transmitters location to inject nanoparticles such that they reach the intended target while avoiding other areas in the body. In this paper, we propose an optimization problem to determine the optimal placement of transmitters to achieve a desired signal strength at a target organ, while ensuring that the interference at the organs we intend to avoid is below a threshold. We consider different scenarios to study how the transmitters location are affected by the desired signal strength for the target, and the threshold interference at the regions to avoid. We find that the choice of the target and avoidance regions, and the model of the circulatory system have a significant impact on the transmitters location.

CCS CONCEPTS

• **Applied computing** → **Biological networks**; • **Theory of computation** → *Mathematical optimization*;

KEYWORDS

Molecular communication, Drug Delivery Systems, Nanonetworks

ACM Reference Format:

Keishla D. Ortiz-Lopez, Mahima Agumbe Suresh, and Radu Stoleru. 2018. Transmitters Location Optimization for Drug Delivery Systems. In *NANOCOM '18: ACM The Fifth Annual International Conference on Nanoscale Computing and Communication, September 5–7, 2018, Reykjavik, Iceland*. ACM, New York, NY, USA, 6 pages. <https://doi.org/10.1145/3233188.3233213>

Permission to make digital or hard copies of all or part of this work for personal or classroom use is granted without fee provided that copies are not made or distributed for profit or commercial advantage and that copies bear this notice and the full citation on the first page. Copyrights for components of this work owned by others than ACM must be honored. Abstracting with credit is permitted. To copy otherwise, or republish, to post on servers or to redistribute to lists, requires prior specific permission and/or a fee. Request permissions from permissions@acm.org.

NANOCOM '18, September 5–7, 2018, Reykjavik, Iceland

© 2018 Association for Computing Machinery.

ACM ISBN 978-1-4503-5711-1/18/09...\$15.00

<https://doi.org/10.1145/3233188.3233213>

1 INTRODUCTION

Drug Delivery Systems (DDSs) play an increasingly important role in providing treatment to major diseases such as cancerous tumors, cardiovascular diseases, diabetes, among others. DDSs have been studied in different fields including biomedical engineering, computer science and medicine. Very recently, researchers focused on studying the use of nanoparticles in DDSs due to its ability to cross biological barriers. With today's DDS designs that use nanoparticles, it has been proven that only 1% of nanoparticles are being delivered to the diseased area [17]. Therefore, optimization of drug delivery using DDSs is of utmost importance.

DDSs with nanoparticles in biomedical engineering and computer science have mostly been studied under the molecular communication (MC) paradigm [2, 4, 6, 7, 9, 11]. In MC, the information is encoded as molecules, where transmitters (e.g. bio-nanomachines, injection devices, etc.) transmit nanoparticles, which are propagated through a channel (e.g., water, air, blood). The MC paradigm models bio-nanomachines and injection devices as transmitters, nanoparticles as the molecular signal, and the targeted site (e.g. organs) as receivers. The transmission of the drug (in the form of nanoparticles) is modeled as propagation model and path loss. This approach simplifies the study of the movement of drugs through the complex human cardiovascular system.

There is work that focuses on the optimal delivery of nanoparticles to the diseased organ by using an active targeting approach [4, 6, 7, 9, 11], in which nanoparticles are directly delivered to targeted organ by using bio-nanomachines acting as transmitters and receivers. On the other hand, the work by Chahibi *et al.* [2, 3] studies the optimal delivery of nanoparticles using a passive targeting approach, where the nanoparticles are injected into the cardiovascular system reaching the targeted site by advection and diffusion. However, none of the mentioned research optimize the locations at which the nanoparticles are injected.

It is important to optimally choose the injection points for the drug. When the drug is inserted into the veins, it flows along with the blood and reaches the heart. It is then diluted and delivered to the organs. Therefore, only a small percentage of the drug reaches the targeted organ. In MC terms, the path loss between the transmitter and receiver is high. If the drug is inserted in the arteries, a small amount is sufficient. Again, in MC terms, as the distance between the transmitter and receiver is reduced, so is the path loss. Inserting drugs directly into the arteries can be dangerous. Hence, it is important to optimally choose the points of injection and the dosage at those points, i.e., the transmitter locations and their transmit powers.

The propagation of the nanoparticles through the human circulatory system resembles the movement of sensors in other flow-based systems such as water distribution systems [12–15]. Such models offer insights on the dissipation models for DDSs. In this paper, we

apply concepts from flow-based systems to model the dissipation of nanoparticles through the blood vessels. We also aim to optimize the number of transmitters (i.e., injection points) and the transmit power (i.e., dosage) such that the receiver (i.e., diseased areas) receives a minimum received signal strength (i.e., drug nanoparticles) while ensuring that the interferences at the other receivers is below a threshold (i.e., side effects in other parts of the body are reduced). Specifically, the main contributions of this paper are the following:

- We formulate the problem as a transmitter placement optimization problem in order to determine the location and transmit power of transmitters (i.e., nanoparticle injectors) in order to ensure a required received signal strength at the desired receivers (target organs), and an interference below a threshold at other receivers (organs to avoid).
- We model the path loss of the human circulatory system through a discrete drug dissipation matrix.
- We solve the MC optimization problem for different scenarios, where the nanoparticles target certain organs, while avoiding certain areas that might be affected by them.

This paper is structured as follows: Section 2 introduces the model and formally presents the optimization problem, whereas Section 3 describes the model. Section 4 presents numerical results for the model under different scenarios, and Section 5 concludes the paper and presents directions for future work.

2 PRELIMINARIES AND PROBLEM FORMULATION

In this section, we define and formulate the optimization problem to determine the location and transmit power of transmitters where nanoparticles need to be deployed.

We consider a DDS that treats diseases throughout the cardiovascular system with multiple transmitters whose task is to inject the nanoparticles in certain locations in the body closer to the diseased area. The MC interpretation of this system is that there are multiple transmitters, and a set of target receivers.

2.1 Definitions

We model the arteries of the human circulatory system as: a) a directed tree $G(V, E)$, in which every edge $(u, v) \in E$ has a non-negative real-valued capacity denoted by $c(u, v)$; and b) two sets of vertices $S = \{s_1, s_2, \dots, s_k\}$ - a set of sources, and $D = \{d_1, d_2, \dots, d_k\}$ - a set of sinks, where $S, D \subset V$. The human circulatory system model is key to the propagation model for the nanoparticles. The movement of the nanoparticles through the human circulatory system is modeled as an acyclic flow network.

Definition 2.1. An Acyclic Flow Network, \mathcal{F} , is defined as a real valued function $\mathcal{F} : \mathcal{V} \times \mathcal{V} \rightarrow \mathbb{R}$ with the following properties:

- $\mathcal{F}(u, v) \leq c(u, v)$, where $c(u, v)$ is a constant indicating the capacity of the edge. This means that the flow on an edge, cannot exceed its capacity.
- $\sum_{w \in V} \mathcal{F}(u, w) = \sum_{w \in V} \mathcal{F}(w, u) \forall u \in V$, unless $u \in S$ or $w \in D$, which means that the net flow of a vertex is 0, except for source and sink nodes.

- Each edge between vertex i and j in \mathcal{F} is an artery, which we assume is an asymmetric cylindrical tube with the following properties:
 - A length l_{ij} .
 - Radii r_{ij}^{top} and r_{ij}^{bot} for the two ends of the artery, and an average radius r_{ij} , which is defined as $r_{ij}^{top} e^{-k_{ij} l_{ij}}$, where $k_{ij} = \frac{\log(r_{ij}^{top}/r_{ij}^{bot})}{l_{ij}}$.
 - A cross-sectional area S_{ij} , where $S_{ij} = \pi r_{ij}^2$.
 - A mean velocity of blood flow u_{ij} .

Definition 2.2. A Zone of Interest (I_t) is a subset of vertices in graph $G(V, E)$, i.e., $I_t \subset V$, which we are interested in delivering the drug to, i.e., the target receivers. For certain diseases, \mathcal{F} may have multiple zone of interest.

The decision vector for each targeted vertex i is defined as $\mathbf{I}_t = [0, 1, 0, \dots,]$, where an entry is equal to 1 if $v_i \in I_t$, 0 otherwise.

Definition 2.3. A Zone of Avoidance (I_a) is a subset of vertices in graph $G(V, E)$, i.e., $I_a \subset V$, which might receive some nanoparticles, but they are not the target receivers. Similar to I_t , a given \mathcal{F} can have multiple zones of avoidance.

The decision vector for each vertex that needs to be avoided is defined as $\mathbf{I}_d = [0, 1, 0, \dots,]$, where an entry is equal to 1 if $v_i \in I_a$, 0 otherwise.

Definition 2.4. The Degree of Coverage of Target (D_{ct}) is the received signal strength threshold of zone I_t . Every receiver in I_t should receive at least D_{ct} fraction of the transmit power (i.e., injected nanoparticles).

Definition 2.5. The Degree of Coverage of Avoidance Organ (D_{ca}) is a threshold interferences in zone in I_a . Every receiver in I_a receives at most D_{ca} fraction of the transmit power (i.e., injected nanoparticles).

Definition 2.6. The decision vector \mathbf{I} is defined as $\mathbf{I} = [0, 1, 0, \dots,]$, where an entry is greater than 0 and at most 1 if a transmitter is present at vertex i , 0 otherwise. The value of \mathbf{I}_i represents the transmit power.

Definition 2.7. The MC propagation model uses a drug dissipation matrix \mathbf{D} , defined such that each element d_{ij} represents how the drug propagates in each artery ij .

$$\begin{bmatrix} d_{11} & d_{12} & \dots & d_{1n} \\ \dots & d_{ij} & \dots & \\ d_{n1} & \dots & \dots & \dots \end{bmatrix}$$

d_{ij} provides the fraction of the drug that reaches vertex v_i if the drug is injected in a vertex v_j . This is the path loss observed by a receiver at v_j if the transmitter is at v_i .

Definition 2.8. The height of each vertex is defined as the length of the path from the root (i.e., heart) to the vertex, which is represented with the vector $\mathbf{H} = [h_1, h_2, \dots, h_i, \dots, h_n]$.

Definition 2.9. The received power in an vertex is defined as the vector $\mathbf{R} = [r_1, \dots, r_i, \dots, r_n]$, which is calculated as follows: $r_j = \sum_{i=1}^n (\mathbf{I}_i \cdot \mathbf{D}_{ij})$.

2.2 Problem Formulation

Given the above definitions, we formulate the optimization problem, which we call the “Transmitter Placement Problem.” The objective of optimization problem is to minimize the *cost* of transmitters placement.

Transmitter Placement Problem: Given an acyclic flow network \mathcal{F} , zones of interest I_t and zones of avoidance I_a in \mathcal{F} where $I_t \cap I_a = \emptyset$, and two degrees of coverage D_{ct} and D_{ca} , find the set $S = \{(s_i, q_i) | s_i \in V \cap q_i \in \mathbb{N}\}$ of transmitters s_i (sources) and their transmit power q_i such that the received signal strength at I_t is at least D_{ct} and the interference at I_a is at most D_{ca} . This problem is mathematically formulated as:

$$\begin{aligned} & \text{minimize} && \sum_{i=1}^n e^{\mathbf{H}_i} \cdot \mathbf{I}_i \\ & \text{subject to:} && \mathbf{I}_t^T \cdot \mathbf{R} \geq D_{ct} \\ & && \mathbf{I}_d^T \cdot \mathbf{R} \leq D_{ca} \\ & && \sum_{i=1}^n \mathbf{I}_i = 1 \end{aligned}$$

We select an exponential function to express the difficulty of placing transmitters as their locations get farther away from the heart. In this paper, we assume that it gets exponentially harder to inject nanoparticles in deeper arteries since blood in arteries is conveyed from the heart to all parts of the body.

We formulate two versions of the optimization problem: **OPT1** and **OPT2**. In **OPT1**, the decision variable \mathbf{I} is set as a binary variable. In **OPT2**, the decision variable \mathbf{I} is set as a real number between 0 and 1.

3 PROPAGATION MODEL FOR NANOPARTICLE DISSIPATION

In this section, we present two models on how the nanoparticles propagate through the cardiovascular system in order to calculate the received power in each vertex in \mathcal{F} . Contrary to radio propagation models where the path loss is a function of distance, the path loss in MC is a function of the dissipation of the nanoparticles through the human circulatory system. As defined in Section 2, the drug dissipation matrix \mathbf{D} provides the path loss function.

One of the most commonly used models was inspired by the work in [8] that also takes a graph-based approach to model the transport of nanoparticles over a network subject to advection and diffusion. The model proposed assumes that the concentration of nanoparticles varies over time and reaches a steady state after a long period of time. An approximation of the model can be obtained by assuming that the concentration is in a steady state. However, their model does not provide a direct way to obtain the fraction of the nanoparticles that reaches an artery if they are injected in a particular artery. Thus, we approximate the drug propagation using simpler models for the following reasons:

- The matrix used to model the drug dissipation needs to be inverted in order to obtain the final concentration, but it cannot be inverted under all conditions.
- The circulatory system takes a long time to achieve a steady state.

In this paper, as an alternative approach, we approximate the dissipation matrix \mathbf{D} using two methods: (i) *Volume*, and (ii) *Flow*. We derive these models from the mobility models for free-flowing sensors in flow-based systems [13–15], and water distribution systems [12]. It is important to note that these are probabilistic models for the movement of the nanoparticles in the blood vessels. Extending the methods proposed in [8] and [3] to obtain the \mathbf{D} matrix is not trivial and is beyond the scope of this paper. The aforementioned models are simple and dependent mostly on the physical properties of the blood vessels.

In the *Volume* approximation, we derive \mathbf{D}_{ij} using:

$$\mathbf{D}_{ij} = \mathcal{I} + \mathbf{P} + \mathbf{P}^2 \dots \mathbf{P}^k$$

where \mathcal{I} is the identity matrix, and

$$\mathbf{P}_{ij} = \frac{\text{Volume of artery entering } v_j}{\text{Total volume of all arteries exiting } v_i}$$

if there is an artery between v_i and v_j , and $\mathbf{P}^k = 0$.

The *Flow* approximation is also obtained similarly. The only difference is that in the *Flow* approximation,

$$\mathbf{P}_{ij} = \frac{\text{Blood flow of artery entering } v_j}{\text{Total blood flow of all arteries exiting } v_i}$$

if there is an artery between v_i and v_j .

The interpretation is that the nanoparticles at a junction follow a probabilistic path, where the probability distribution is guided either by the volume of arteries leaving the junction (in the *Volume* approximation), or the blood flowing away from the junction (in the *Flow* approximation).

4 NUMERICAL RESULTS

In this section, we present numerical results to demonstrate the benefit of our optimization model. We have also included a subsection to discuss the interpretation of the results and the practical applications of the model.

We use AMPL to solve the optimization problem for different scenarios on the NEOS solver [5]. In order to model the vertices and edges in \mathcal{F} , we use the anatomical data of large arteries collected in [10] from a young male, where we denote large arteries as the edges and the vertices are the junctions that form each artery. The graph is shown in Figure 1 and the list of large arteries and their dimensions are shown in Table 1.

We evaluate our model for both the *OPT1* and *OPT2* objectives with both the *Volume* and *Flow* approximation models. The metrics we used are: (i) Cost - the cost function $\sum_{i=1}^n e^{\mathbf{H}_i} \cdot \mathbf{I}_i$, described in Section 2.2, (ii) Number of transmitters, and (iii) Location of transmitters. The parameters we changed in our analysis are: (i) D_{ct} from 0.3 to 0.6 in increments of 0.1; (ii) D_{ca} from 0.02 to 0.1 in increments of 0.02; (iii) Scenario.

The different scenarios used in the evaluation are shown in Table 2. In each scenario, we consider different target arteries and the same avoidance arteries, which are identified by the vertices that form a specific artery we aim to target or avoid. The reason to select the same avoidance arteries for all scenarios is because splenic

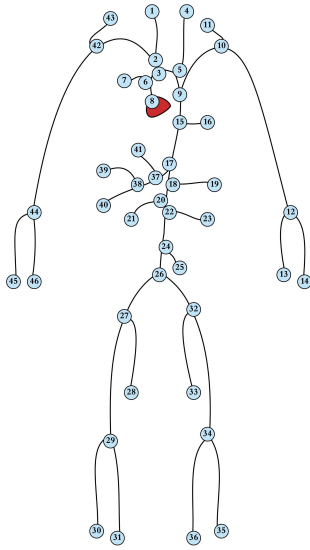


Figure 1: Topology of large arteries with vertices labeled.

Table 1: List of edges (large arteries) and their dimensions.

Edge ij	Name	ℓ_{ij} (cm)	r_{ij}^{sup} (cm)	r_{ij}^{bot} (cm)
(8,6)	Ascending aorta	1	1.525	1.502
(6,3)	Ascending aorta	3	1.502	1.42
(3,5)	Aortic arch	3	1.42	1.342
(5,9)	Aortic arch	4	1.342	1.246
(9,15)	Thoracic aorta	5.5	1.246	1.124
(15,17)	Thoracic aorta	10.5	1.124	0.924
(17,18)	Abdominal aorta	5.25	0.924	0.838
(18,20)	Abdominal aorta	1.5	0.838	0.814
(20,22)	Abdominal aorta	1.5	0.814	0.792
(22,24)	Abdominal aorta	12.5	0.792	0.627
(24,26)	Abdominal aorta	8	0.627	0.55
(26,27),(26,32)	External iliac	5.75	0.4	0.37
(27,29),(32,34)	Femoral	14.5	0.37	0.314
(29,31),(34,36)	Femoral	44.25	0.314	0.2
(27,28),(32,33)	Internal iliac	4.5	0.2	0.2
(29,30),(34,35)	Deep femoral	11.25	0.2	0.2
(6,7)	Coronaries	10	0.35	0.3
(3,2)	Brachiocephalic	3.5	0.95	0.7
(2,42),(9,10)	Subclavians	3.5	0.425	0.407
(42,44),(10,12)	Brachials	39.75	0.407	0.25
(44,45),(12,14)	Radials	22	0.175	0.175
(44,46),(12,13)	Ulnars	22.25	0.175	0.175
(42,43),(10,11)	Vertebrals	13.5	0.2	0.2
(2,1)	R. carotid	16.75	0.525	0.4
(5,4)	L. carotid	19.25	0.525	0.4
(15,16)	Intercostals	7.25	0.63	0.5
(18,19)	Sup. mesenteric	5	0.4	0.35
(17,37)	Celiac	2	0.35	0.3
(37,38)	Hepatic	2	0.3	0.25
(37,41)	Hepatic	6.5	0.275	0.25
(38,40)	Gastric	5.75	0.175	0.15
(38,39)	Splenic	5.5	0.2	0.2
(20,21),(22,23)	Renals	3	0.275	0.275
(24,25)	Mesenteric	3.75	0.2	0.175

and hepatic supply to the spleen and liver respectively which are clearance organs [1].

The cost function at the optimal solution with the *Flow* approximation, for *OPT1* are shown in Figure 2, and for *OPT2* are shown in Figure 3. For Scenario 3, we see infeasible solutions for all values of D_{ct} and D_{ca} with *OPT1* with *Flow* approximation. We observe that the cost increases as D_{ct} increases, and decreases as D_{ca} increases. It means that as we need more receiver signal strength at the target

Table 2: Scenarios used for numerical results where avoidance arteries (I_a) are hepatic (37,38,41) and splenic (38,39).

Scenario #	Target (I_t)
1	Abdominal aorta (24,26)
2	Sup. mesenteric: (18,19), Renals: (20,21,22,23)
3	Sup. mesenteric: (18,19)
4	Femorals: (27,29,32,34)

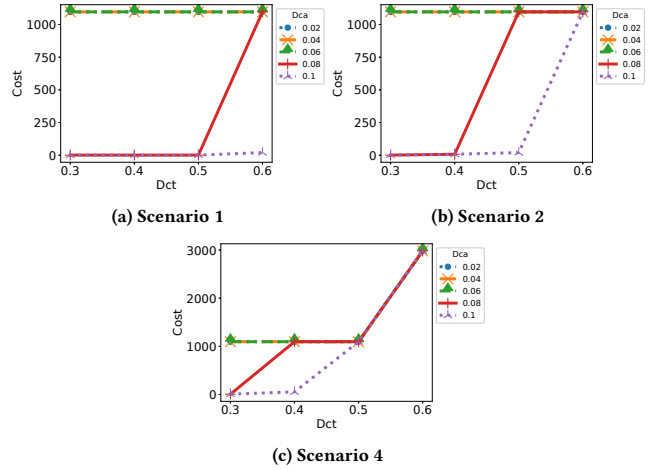


Figure 2: Optimal Cost in some scenarios with *OPT1* and *Flow* approximation model for different values of D_{ct} and D_{ca} .

organ, or less interference at the avoidance organs, the cost to do so increases. The way the cost increases in each scenario, however, it is different.

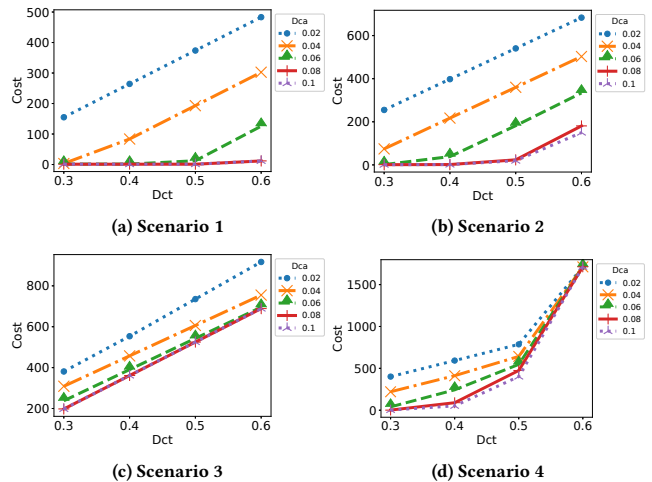


Figure 3: Optimal Cost in each scenario with *OPT2* and *Flow* approximation model for different values of D_{ct} and D_{ca} .

The cost function at the optimal solution with the *Volume* approximation, for *OPT1* are shown in Figure 4, and for *OPT2* are

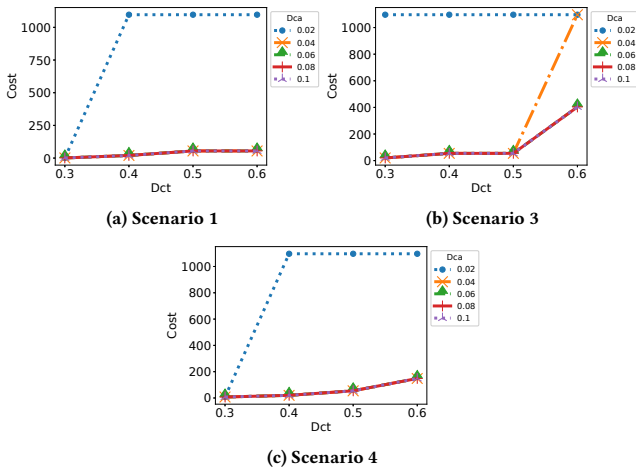


Figure 4: Optimal Cost in some scenarios with *OPT1* and *Volume* approximation model for different values of D_{ct} and D_{ca} .

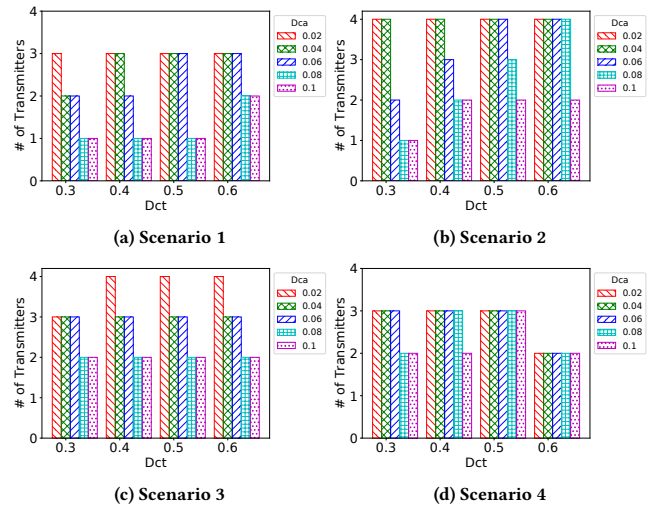


Figure 6: Number of transmitters in each scenario with *OPT2* and *Flow* approximation model for different values of D_{ct} and D_{ca} .

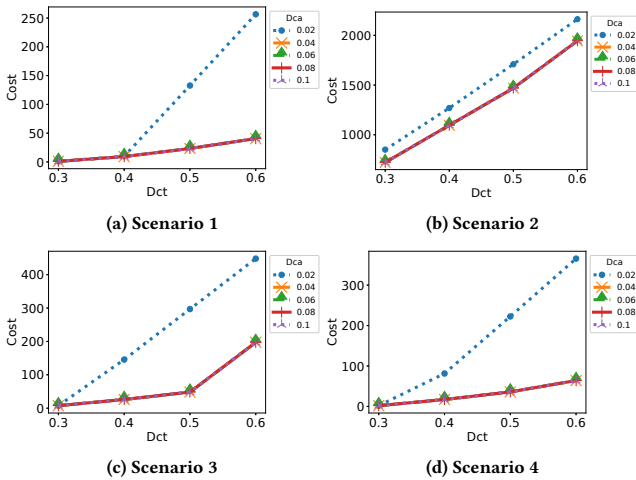


Figure 5: Optimal Cost in each scenario with *OPT2* and *Volume* approximation model for different values of D_{ct} and D_{ca} .

shown in Figure 5. The results show similar trends as the *Flow* approximation model. However, Scenario 2 has an infeasible solutions with the *Volume* approximation for *OPT1*. Also, D_{ca} has lesser effect on the cost as compared to the *Flow* approximation.

The number of transmitters at the optimal solution with the *Flow* and *Volume* approximation for *OPT2* are shown in Figures 6, and 7. For *OPT1*, the number of transmitters is always 1, if there is a feasible solution. The results show that in most cases, the number of transmitters either increases or stays the same as D_{ct} is increased and D_{ca} is decreased.

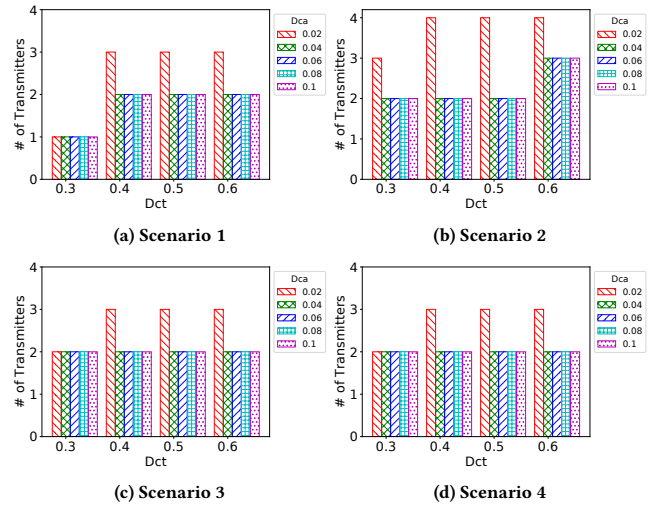


Figure 7: Number of transmitters in each scenario with *OPT2* and *Volume* approximation model for different values of D_{ct} and D_{ca} .

4.1 Result interpretation and Discussions

Present work in DDSs shows that if all the drug is injected in the veins (i.e., distributed by the heart), less than 1% of the drug reaches the targeted organ. Compared to that, our solutions improve the result by injecting the drug in the arteries.

The choice of regions to target and avoid has a huge impact on the transmitter locations and cost. We see that sometimes the number of transmitters changes when D_{ca} is changed for a given D_{ct} , and vice versa, but they remain the same in several cases. From

D_{ct} \ D_{ca}	0.02	0.04	0.06	0.08	0.1
0.3	8, 18, 21, 7	8, 18, 21, 7	8, 7	8	8
0.4	8, 18, 21, 7	8, 18, 21, 7	8, 21, 7	8, 5	8, 5
0.5	8, 18, 21, 7	8, 18, 21, 7	8, 18, 21, 5	8, 5, 21	8, 5
0.6	8, 18, 21, 7	8, 18, 21, 5	8, 18, 21, 5	9, 19, 21, 5	9, 21

D_{ct} \ D_{ca}	0.02	0.04	0.06	0.08	0.1
0.3	8, 18, 7	8, 18, 7	8, 18, 7	8, 5	8, 5
0.4	8, 18, 7	8, 18, 5	8, 18, 5	9, 18, 5	9, 5
0.5	8, 18, 5	9, 18, 15	17, 18, 15	17, 18, 15	17, 18, 15
0.6	18, 20	18, 20	18, 20	18, 20	18, 20

Table 3: Transmitter locations for scenarios 2 and 4 respectively with OPT2 and Flow approximation model for each D_{ct} and D_{ca} combination.

Table 3, we see that although the number stays the same, the specific locations of the transmitters are different. When the transmitter locations change, so does the cost. Therefore, a combination of the cost and number of transmitters gives a better understanding of the difficulty of meeting the requirements.

Additionally, the transmitter placement patterns change at specific points as D_{ct} and D_{ca} are changed. We observe that the received signal strength at the targeted region and the interference at the avoidance region can remain the same over more than one set of D_{ct} and D_{ca} values for the same scenario. This typically occurs when a set of transmitters provides much more than D_{ct} nanoparticles in the targeted region, and much less than D_{ca} nanoparticles in the avoidance region.

There are some cases when the solution is infeasible. If the D_{ct} is too large, or the D_{ca} is too small, it becomes increasingly harder to satisfy the constraints. Beyond a certain limit, the problem becomes infeasible, e.g., requiring all of the drug to be delivered to two organs is not possible. In other circumstances that are not as severe, infeasibility occurs due to the way the dissipation happens. The point at which the infeasible solution occurs is also not the same across scenarios and dissipation models.

Another interesting observation is that the results are different for the Volume and Flow approximation models. This shows the importance of the blood circulation model for this problem. This highlights the importance of an accurate model for the blood circulation system.

These observations show that the transmitter locations depend heavily on the disease, human body condition, and the coverage requirements.

5 CONCLUSIONS AND FUTURE WORK

In this paper, we have presented the Transmitter Placement Problem in order to determine the optimal location and transmit power of transmitters in the human cardiovascular system to ensure a required received signal strength at the desired receivers, and an interference below a threshold at other receivers. We proposed two approximation propagation models based on blood flow and volume of large arteries. To evaluate both models, we consider four scenarios with different targets and same avoidance areas to study how the transmitter locations are affected by the desired signal strength for the target and the threshold interference at the regions to avoid. Results showed that the transmitters location depend on

the location of the disease, propagation models, and the received signals requirement at the receivers.

This work opens up several new avenues to make the optimization problem more realistic. An important extension that we leave for future work is to consider the continuous cyclic movement of the nanoparticles in the human circulatory system. Furthermore, the drug dissipation models used in this paper are approximations, and real models validated through simulations, or mathematical models need to be developed. Deriving from related work in flow-based systems [16], we envision a bio-medical cyber-physical system approach to the DDS by including a control system to vary the dosage at transmitters location.

ACKNOWLEDGMENTS

This work was supported by NSF grant 1253968. We would like to thank the anonymous reviewers for their feedback.

REFERENCES

- [1] A. C. Anselmo, V. Gupta, B. J. Zern, D. Pan, M. Zakrewsky, V. Muzykantov, and S. Mitragotri. 2013. Delivering Nanoparticles to Lungs while Avoiding Liver and Spleen through Adsorption on Red Blood Cells. *ACS Nano* 7, 12 (2013), 11129–11137.
- [2] Y. Chahibi, M. Pierobon, and I. F. Akyildiz. 2015. Pharmacokinetic Modeling and Biodistribution Estimation Through the Molecular Communication Paradigm. *IEEE Transactions on Biomedical Engineering* 62, 10 (Oct. 2015), 2410–2420.
- [3] Y. Chahibi, M. Pierobon, S. O. Song, and I. F. Akyildiz. 2013. A Molecular Communication System Model for Particulate Drug Delivery Systems. *IEEE Transactions on Biomedical Engineering* 60, 12 (Dec. 2013).
- [4] Y. Chen, Y. Zhou, R. Murch, and P. Kosmas. 2017. Modeling Contrast-Imaging-Assisted Optimal Targeted Drug Delivery: A Touchable Communication Channel Estimation and Waveform Design Perspective. *IEEE Transactions on Nanobioscience* 16, 3 (April 2017), 203–215. <https://doi.org/10.1109/TNB.2017.2669309>
- [5] E. D. Dolan, R. Fourer, J. J. Moré, and T. S. Munson. 2002. Optimization on the NEOS Server. *SIAM News* 35, 6 (2002), 4.
- [6] L. Felicetti, M. Femminella, and G. Reali. 2017. Congestion Control in Molecular Cyber-Physical Systems. *IEEE Access* 5 (2017), 10000–10011.
- [7] M. Femminella, G. Reali, and A. V. Vasilakos. 2015. A Molecular Communications Model for Drug Delivery. *IEEE Transactions on Nanobioscience* 14, 8 (2015), 935–945.
- [8] L. LM Heaton, E. López, P. K. Maini, M. D. Fricker, and N. S. Jones. 2012. Advection, diffusion, and delivery over a network. *Physical Review E* 86, 2 (Aug. 2012), 021905.
- [9] T. Nakano, Y. Okaie, and A. V. Vasilakos. 2013. Transmission Rate Control for Molecular Communication among Biological Nanomachines. *IEEE Journal on Selected Areas in Communications* 31, 12 (Dec. 2013), 835–846.
- [10] M. S. Olufsen, C. S. Peskin, W. Y. Kim, E. M. Pedersen, A. Nadim, and J. Larsen. 2000. Numerical Simulation and Experimental Validation of Blood Flow in Arteries with Structured-tree Outflow Conditions. *Annals of Biomedical Engineering* 28, 11 (2000), 1281–1299.
- [11] S. Salehi, N. S. Moayedian, S. S. Assaf, R. G. Cid-Fuentes, J. Solé-Pareta, and E. Alarcón. 2017. Releasing Rate Optimization in a Single and Multiple Transmitter Local Drug Delivery System with Limited Resources. *Nano Communication Networks* 11 (March 2017), 114–122. <https://doi.org/10.1016/j.nancom.2017.03.001>
- [12] M.A. Suresh, L. Smith, A. Rasekh, R. Stoleru, M.K. Banks, and B. Shihada. 2014. Mobile Sensor Networks for Leak and Backflow Detection in Water Distribution Systems. In *IEEE 28th International Conference on Advanced Information Networking and Applications (AINA)*.
- [13] M.A. Suresh, R. Stoleru, R. Denton, E. Zechman, and B. Shihada. 2012. Towards Optimal Event Detection and Localization in Acyclic Flow Networks. In *Distributed Computing and Networking (ICDCN)*.
- [14] M.A. Suresh, R. Stoleru, E.M. Zechman, and B. Shihada. 2013. On Event Detection and Localization in Acyclic Flow Networks. *IEEE Transactions on Systems, Man, and Cybernetics: Systems* 43, 3 (2013).
- [15] M.A. Suresh, W. Zhang, W. Gong, A. Rasekh, R. Stoleru, and M.K. Banks. 2015. Towards Optimal Monitoring of Flow-based Systems using Mobile Wireless Sensor Networks. *ACM Transactions on Sensor Networks* 11, 3 (2015).
- [16] M. A. Suresh, U. Manohar, A. G. R. R. Stoleru, and M. Kumar M S. 2014. A Cyber-Physical System for Continuous Monitoring of Water Distribution Systems. In *IEEE 10th International Conference on Wireless and Mobile Computing, Networking and Communications (WiMob)*.
- [17] A. Trafton. 2009. Tumors Targeted using Tiny Gold Particles. *MIT Tech Talk* 53 (2009), 4.